

Chapter 3

Optical Remote Sensing in Lake Trasimeno: Understanding from Applications Across Diverse Temporal, Spectral and Spatial Scales



Bresciani Mariano, Free Gary, Pinardi Monica, Laanen Marnix, Padula Rosalba, Fabbretto Alice, Mangano Salvatore, and Giardino Claudia

Abstract Under the current Anthropocene Epoch there is an urgent need to deliver high-quality data, information and knowledge to the decision-making process for a sustainable management of environmental concerns, in particular for inland water. Most literature address the advantages brought by remote sensing (RS) techniques in operational monitoring and management of lakes. In the present work, optical RS is applied to a complex ecosystem, the turbid eutrophic shallow Lake Trasimeno (Italy). A first example of RS application addresses the use of high frequency spectroradiometric measurements collected by a WISPstation to retrieve intra-inter daily and seasonal dynamics of chlorophyll-a and phycocyanin. A second section focuses on long term trends of water quality by means of satellite data time series for the whole lake surface. Then we exploit the latest generation of hyperspectral satellite images (PRISMA and DESIS) utilizing the high spectral resolution and improving the accuracy of estimated lake water quality. Finally, high spatial resolution satellite data is used for a finer scale mapping of bottom substrates. Application of these techniques improved scientific understanding on the timing, composition and distribution of phytoplankton blooms, the role of nutrients and climate drivers as well as changes in the extent and composition of aquatic plants.

B. Mariano (✉) · F. Gary · P. Monica · F. Alice · M. Salvatore · G. Claudia
Institute for Electromagnetic Sensing of the Environment, National Research Council, Via Bassini
15, 20133 Milan, Italy
e-mail: bresciani.m@irea.cnr.it

L. Marnix
Water Insight, Marijkeweg 22, 6709 PG Wageningen, The Netherlands

P. Rosalba
ARPA UMBRIA, Via Pievaiola, 207/B-3 Loc. S. Sisto, 06132 Perugia, Italy

3.1 Introduction

A key message of the Organization for Economic Cooperation and Development's (OECD) Environmental Strategy for the first decade of the twenty-first century to address environmental sustainability was to improve information available for decision making by measuring progress using quality indicators; for water quality of lakes and rivers, in particular, the progress made is still insufficient [1]. Reasonable management of some of the world's most serious environmental problems depends on the delivery of high-quality data, information and knowledge to the decision-making process [2]. Data quality comprises components of relevance, reliability, accuracy, accessibility, timeliness, interpretability and coherence [3]. For the freshwater ecosystems in Europe, the EU Water Framework Directive (WFD) is an ambitious legislation framework, which collects all information on the state of water in order to verify the commitment of the different countries to preserve water resources and to achieve a good state of water quality [4]. Substantial progress has been made in the past 30 years in understanding the causes of both water scarcity and water quality degradation, as well as in developing effective strategies to prevent or mitigate its adverse effects [5–7]. However, this is still not enough, especially if we consider emerging pressures such as global warming and climate change, which alter ecosystems dynamics and makes understanding and modelling more challenging.

In particular, many studies have highlighted how lakes are ecosystems of particular importance for the assessment of already ongoing climate change [8, 9] and the need of large data-sets to provide more information that can lead to a capacity for understanding and the management of current and future issues.

Since 1991, Bukata et al. [10] suggested that satellite monitoring of optically-active components of inland water is an essential input to studies addressing the impact of climate change; since this first contribution, several other scientific articles pointed out the importance of satellite data for monitoring water quality of lakes with particular focus on the relationship with climate change (e.g., Yang et al. [11]). In fact, satellite remote sensing can provide near-real time, synoptic, and repeated data for monitoring physical and biogeochemical parameters of water status that avoids interpretive problems associated with spatial and temporal under sampling of traditional limnological field campaigns. Indeed, over the last three decades, there has been a significant advancement in the development of both technology and algorithms that allow the monitoring via satellite of ocean color to be used for studying coastal and ocean water quality [12]. Earth observation (EO) data acquired by satellites is increasingly used for providing information on a suite of functionally relevant indicators of water quality and ecosystem conditions from a local to global scale [13]. In the most recent review articles [14–18], robustness and maturity of remotely sensed based monitoring of the lakes have been addressed in terms of sensors availability, data quality, variability and consistency of processing algorithms, validation and accuracy assessment of the output products and advantages brought by satellite remote sensing to operational monitoring and the management of lake systems.

In this chapter, we present the application of EO techniques to the case study of Lake Trasimeno (Italy), a turbid eutrophic shallow lake. In order to provide an exhaustive description of the potential of EO data for monitoring aquatic environments, we divided the chapter into four sections. Section 3.3 First, we present the use of data acquired by a WISPstation, an in situ fixed spectroradiometer, for continuous point monitoring with high temporal frequency that can depict sub-hourly, daily and seasonal dynamics of lake water quality; these reflectance measurements can also be exploited for the validation of satellite data processing. Section 3.4 focuses on the relevance of time series of satellite data for the analysis of long term trends and inter-annual dynamics of the status of lake water with a synoptic view over the whole lake surface based on data produced by the Lakes Climate Change Initiative (CCI) project. Section 3.5, we present the characteristics of the latest generation of hyperspectral satellite images as exploited for deriving high accuracy and up-to-date information on lake water status that can be achieved as a result of the high spectral resolution offered by these sensors. Section 3.6 focuses on the opportunities offered by satellite and/or airborne sensors that acquire data with very high spatial resolution for a finer spatial analysis of water surface optical properties. Based on the applications presented in this chapter, we can draw the conclusion that synoptic view, high temporal frequency of observation, high spatial and spectral resolution offered by RS techniques constitute a unique source of information for monitoring complex ecosystem such as Lake Trasimeno.

3.2 Study Area

This study focuses on Lake Trasimeno, a post-tectonic, shallow (maximum depth 6.3 m), located in central Italy (43°08'N; 12°06'E; Fig. 3.1). It is the fourth largest lake of the country (average surface area 120.5 km² with a circular shape) with three small islands (Polvese, Maggiore and Minore islands) and has an extensive bay—Oasi la Valle that is colonized by aquatic vegetation in the south-east [19]. Nearly all the littoral zones of Trasimeno are colonized by aquatic vegetation mainly composed by helophytes (e.g. *Phragmites australis*, *Typha angustifolia*), and hydrophytes (e.g. *Potamogeton pectinatus*, *Chara globularis*, *Myriophyllum spicatum*) [20].

Lake Trasimeno is of significant conservation importance and is part of a Natural Regional Park, Site of Community Interest, Special Protection Zone and of two Natura 2000 sites (IT5210018 and IT5210070) [21].

The catchment of Lake Trasimeno lies over a substratum of low permeability (turbidite), covered by Plio-Pleistocene and Holocene deposits, with a variable content of silicatic and of carbonatic minerals [22, 23]. However, despite their low permeability, these formations host small aquifers [22] where all the infiltrating water radially flows towards the lake [24]. Because of the small area of the catchment relative to the lake area, the annual water inflows are frequently lower than evaporation losses and the water balance of the lake is therefore strongly affected by the pluviometric regime [23] and by the extreme variability of the climate that

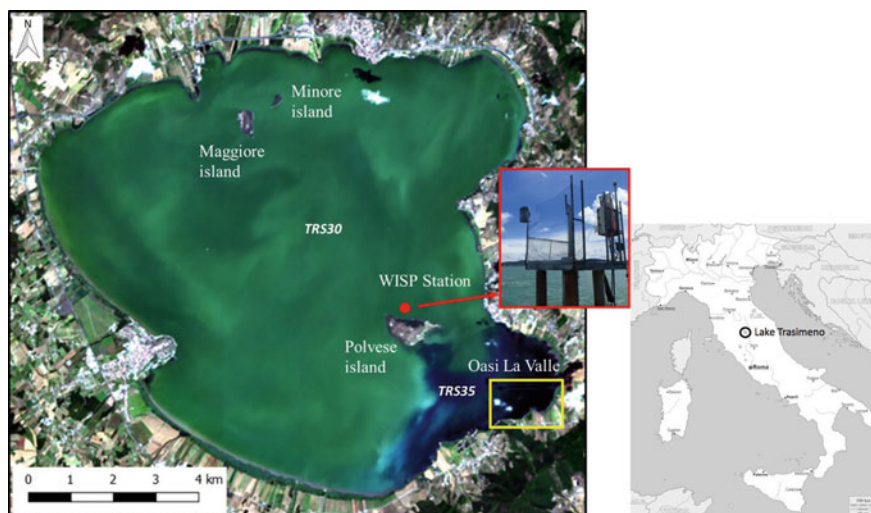


Fig. 3.1 True color composition of Lake Trasimeno from satellite (PRISMA data acquired on 25 July 2020) and its location in Italy. The image shows the WISPstation position (red dot) and the Oasi La Valle bay colonized by macrophytes (yellow box). Inset (red box) is a picture of the platform supporting the WISPstation. The ARPA Umbria stations (TRS30 and TRS35) used for WFD monitoring are also indicated

characterizes the Mediterranean area. In the past, the lake was subject to human interventions on inflows and outflows in order to regulate the lake level since Etruscan or Roman times [21, 23]. A dramatic hydrological crisis occurred in the 1950s due to the artificial outflow threshold being displaced after its restructuring at the end of the nineteenth century [25]. Following the enlargement of the catchment area the lake level increased from 1960 to 1965, followed by an alternation of wet and drought periods. In order to prevent flooding of the coastal area, on one occasion in 2015, the artificial outlet was opened for some days after being closed for about 30 years [24]. Under the current climate change scenario, the lake level is in a low phase and the rules restricting abstraction together with the maintenance works on the inflowing rivers seem to be insufficient to avoid the significant reduction in water availability [25]. During drought periods, higher concentrations of suspended solids, an accumulation of dissolved salts and an increase of the total alkalinity can occur [26].

The consequences of the periodically low water levels have had a negative effect on the entire ecosystem, in terms of impoverishment of native biodiversity and reduced fishing yield; these effects are exacerbated by water abstractions for irrigation purposes and by the presence of civil and agricultural discharges [21]. Tourism, fisheries and agriculture (cultivated lands cover about 70% of the catchment) are the most important activities in the Trasimeno area.

Lake Trasimeno is generally turbid (average Secchi disk depth 1.1 m and the average total suspended matter was 10.4 gm^{-3} for the period 2002–2008) and in

meso-eutrophic conditions with chlorophyll-a (Chl-a) concentration up to 90 mg m^{-3} [21, 27]. The water column is unstratified, with recurring sediment resuspension as a result of wind action. According to the WFD, the lake is currently classified at moderate ecological status [28].

Lake Trasimeno has a phytoplankton community dominated by chlorophytes and dinoflagellates. Cryptophytes also comprised a relatively large portion of the biomass, whereas euglenophytes and diatoms are relatively scarce [29]. The high nutrient concentrations favor the occurrence of phytoplankton blooms, including cyanobacteria species (e.g. *Cylindrospermopsis raciborskii*, *Planctothrix agardhii*) [26, 30]. The zooplankton is dominated by cyclopoids tending to have the greatest relative biomass in autumn, and Cladocera with peaks in winter or spring [29].

The fish community of Lake Trasimeno comprises 19 species and is dominated by cyprinids [31]. The most important commercial native fish species in the lake are tench (*Tinca tinca*), southern pike and eel (*Anguilla Anguilla*). The remarkable decline of tench, and other native species, coincided with a substantial expansion of the alien goldfish (*Carassius auratus*) [31].

3.3 High Frequency Spectroradiometric Measurements

Phytoplankton responds to changes in environmental conditions very quickly [32], and phytoplankton growth in Lake Trasimeno is also influenced by both phytoplankton physiology and external factors, including light, temperature, and nutrients. Drivers affecting short-term dynamics in populations and communities are complex and may consist of several factors acting in parallel. Sometimes environmental drivers induce rhythmic oscillations, which are easily linked to recognized important factors such as diurnal shifts in temperature and light [33, 34]. In addition to the high dynamics of phytoplankton, the low lake depth influences the resuspension of the bottom sediments due to wind action. These resuspensions determine the typical turbid water conditions for Lake Trasimeno. Diurnal and seasonal variation affect the physicochemical variables thereby causing variation in the abundance and diversity of plankton [35] and suspended sediments.

Bresciani et al. [19] recently evaluated the dynamics of the Chl-a concentrations of Lake Trasimeno for six months in 2018, using data gathered from the fixed position autonomous radiometer WISPstation (located 400 m north from the Polvese island as in Fig. 3.1). Briefly, the WISPstation allows continuous measurements with two radiance sensors that look downward to the water surface at an angle of 40° from the vertical (L_{up}) and a sky looking radiance sensor looking upward at an angle of 40° from the vertical (L_{sky}) in the NNW direction and two radiance channels collecting L_{up} and L_{sky} in the NNE direction and two irradiance channels in a wavelength range of 350 to 1100 nm. Data are transmitted to the database (“WISPcloud”) automatically through a cellular connection.

In this work, we develop the analysis of Bresciani et al. [19] by extending the temporal range for Chl-a analysis as well as by adding the analysis of phycocyanin

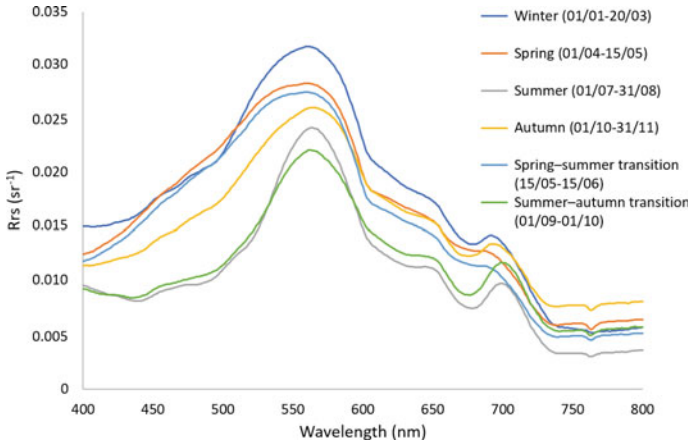


Fig. 3.2 Average Water spectral signatures (remote sensing reflectance, Rrs) from WISPstation data on the six different time intervals for the WFD classification [40]

(PC) derived, as for Chl-a, from the conversion of Remote Sensing Reflectance (Rrs) measured by the WISPstation [36]. Moreover, the hyperspectral Rrs data from the WISPstation enable us to also simulate the band setting of satellite data providing valuable reference data to be compared to satellite observations [37]; an example of using the WISPstation data for this is presented in Sect. 3.5.

The WISPstation Rrs data used in this section were collected continuously from 24th April 2018 to 30th November 2020 every 15 min. Over 30,000 acquisitions of Rrs data with corresponding values of Chl-a and phycocyanin (PC) for water quality monitoring purposes were available for the analysis. The Chl-a was derived through a standard water quality algorithm [38] and for PC retrieval the algorithms of Simis [39].

Figure 3.2 shows average values of Rrs in different periods of the year, selected based on the time interval for the WFD classification [40]. In summer and in summer-to-autumn the effect of phytoplankton on Rrs is evident in the lower values of the blue wavelengths and generates the typical feature of absorbance/reflectance in the region between 665 and 705 nm. In both cases it is also evident the contribution of cyanobacteria pigments in between 625 and 650 nm. In the winter and spring the higher values of Rrs were attributed to both a lower presence of phytoplankton and higher concentrations of Total Suspended Matter (TSM).

Examining the WISPstation data for Chl-a it is interesting that the start and rate of increase of the summer bloom was remarkably similarly in the three investigated years (Fig. 3.3). The increase always began in the first week of July and peaked in September. The rate of increase was linear up until early September (with an $R^2 > 0.8$). In particular, considering the Day of Year (DOY) 180 to 250 (29th June–7th September) the slopes of the increase were 0.54, 0.50 and 0.59 for 2018, 2019 and 2020 respectively and were not significantly different in a linear model (testing year for interaction with DOY or between individual years ($p > 0.05$) [41–43]).

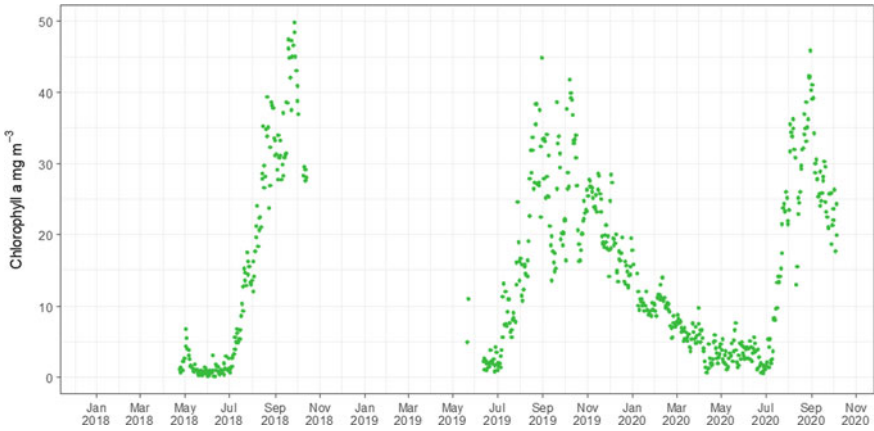


Fig. 3.3 Chlorophyll-a concentration averaged at daily level from the WISPstation data

The WISPstation also produces estimates of the pigment phycocyanin useful for estimating the seasonal dynamics of cyanobacteria. Figure 3.4 shows a plot of Chl-a and phycocyanin concentrations for 2020. It can be seen that sudden increases in Chl-a correspond to sudden increases in phycocyanin. For example from the 1st of August, a rapid increase in Chl-a from 22 to 35 mg m⁻³ over a period of four days corresponds to a period of rapid increase in phycocyanin. Conversely the rapid decline in phycocyanin on the 11th of August is matched by a decline in Chl-a. A similar pattern occurs at the beginning of September where an increase in cyanobacteria drives the Chl-a to its annual maximum level. Utilizing the phycocyanin results from the WISPstation showed how cyanobacteria played a key role in the sudden increases and declines in Chl-a in mid to late summer. Combining Chl-a and phycocyanin data allows managers to see when the composition of blooms is driven by potentially

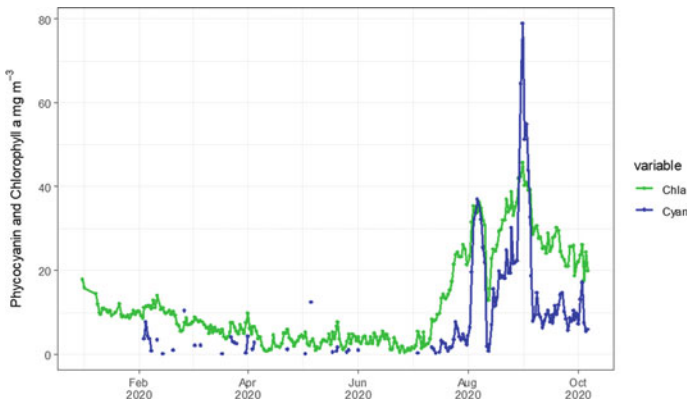


Fig. 3.4 Chlorophyll-a (green) and phycocyanin (blue) pigment concentration averaged at daily level from the WISPstation data

toxic cyanobacteria in almost real time. However, despite the presence of potentially harmful algae, toxicity tests carried out for bathing water purposes have been reported as negative for Trasimeno lake [44].

The high frequency measurements provided by the WISPstation have unique value in improving scientific knowledge and in providing opportunities for improved management for high value recreational lakes like Trasimeno. Examining the timing and rate of bloom development using high frequency data revealed that it was consistent among the three years examined. This predictability provides an opportunity to understand and model the timing and size of blooms for management purposes.

In Italy there are three phases of monitoring in lakes at risk of cyanobacteria blooms: routine, alert and emergency which are differentiated by response (sampling intensity and parameters measured) and management action (ranging from none to risk-communication, scum removal and a bathing ban) in response to increasing health risk [45]. One of the main challenges in the current guidelines is the provision of adequate temporal and spatial monitoring of cyanobacteria. Daily sampling is unfeasible and wind-driven accumulations of cyanobacteria can present dangerous concentrations of toxins within a period of hours [46]. One of the benefits of the WISPstation is that it couples Chl-a and phycocyanin data allowing managers to see when the composition of blooms is driven by potentially toxic cyanobacteria in almost real time and would improve all monitoring phases if incorporated. The drawback is that the WISPstation is limited to a fixed position on the lake.

The mechanisms driving the sudden increase in cyanobacteria detected by the WISPstation are likely to include nutrient inputs, mixing, wind driven accumulations or surface accumulation given their buoyancy and previous work has indicated that these factors are linked to variation in Chl-a [19, 46]. In addition, the drivers in the observed pattern of Chl-a and PC are also likely to be highly dependent on species succession in response to and alongside changing physical and chemical drivers. The rapid changes in Chl-a and PC during the August–September period are typically reflected in highly dynamic changes in the phytoplankton community. For example in 2018, cyanobacteria dominance shifted from *Snowella lacustris* (8th July–5th August) to *Cylindrospermopsis raciborskii* (12th August–10th September) and finally to *Planktothrix agardhii* (16th–24th September) [47]. Such changes in seasonal composition were also indicated by the different spectral signatures over time in Fig. 3.2.

3.4 Long Term EO Data-Set

The European Space Agency's (ESA) climate change initiative (CCI) aims to exploit the long term global earth observation record to produce essential climate variables (ECVs) supporting the United Nations Framework Convention on Climate Change (UNFCCC). The objective of the CCI dataset for the ECV Lakes is to use satellite data to create the largest and longest possible consistent, open global record of five lake

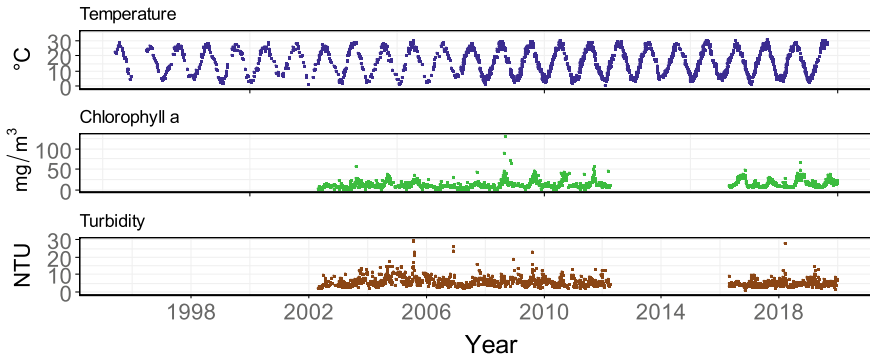


Fig. 3.5 Climate Change Initiative (CCI) results for Lake Trasimeno for LSWT, Chl-a and turbidity from 1996 to 2019

thematic variables: lake water level, extent, temperature, water-leaving reflectance, and ice cover. The main characteristics of this data set [48] are:

- Spatial coverage: 250 globally distributed lakes, set to expand to around 2,000 in the second phase.
- Spatial resolution: 1/120 degree global grid.
- Temporal resolution: daily netCDF files containing all variables and associated uncertainty.
- Temporal coverage: from 1992 up to 2019.

For Lake Trasimeno, lake surface water temperature (LSWT), Chl-a and turbidity (the latter two derived from water-leaving reflectance) were available in the CCI Lakes database version 1.0 (Fig. 3.5). The dataset for LSWT dates from 1993 while that for the other parameters starts in 2002. The increased intensity of satellite monitoring is visible comparing LSWT recorded in the 1990s with that currently. There is a significant data gap in Chl-a and turbidity from 2012 to 2015 due to the failure of the MERIS satellite. One of the current management issues facing Trasimeno lake is eutrophication. The lake can be classified as eutrophic based on Chl-a with seasonal blooms hindering the recreational use of the lake. The peak height of the blooms can be seen to increase from 2008 onwards in Fig. 3.5. The variation in bloom incidence between years can also be seen by plotting the distribution for each year. Figure 3.6 shows a ridge plot for the data where several years are noted to have concentrations above 30 mg m^{-3} . Such blooms typically occur in early to mid-September, only 2003 and 2005 had blooms centered in August in the data analyzed (Fig. 3.5).

The CCI data set presents an opportunity to examine what parameters are important in controlling the size of blooms and their inter-annual variation. In order to do this the Chl-a data were linearly interpolated to daily resolution. The most continuous period 2003–2011 was included for analysis. Few in situ environmental data sets are available to match this temporal resolution so daily climatic data were obtained from ERA5, the fifth generation ECMWF reanalysis for the global climate and

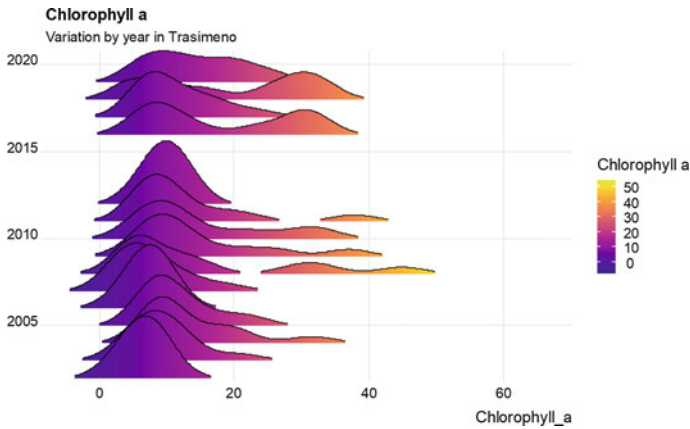


Fig. 3.6 Ridge plot showing distribution of Chl-a concentration mg m^{-3} from 2002 to 2019 for Lake Trasimeno

weather (<https://cds.climate.copernicus.eu/cdsapp#!/home>). Data used in the analysis included: wind direction and speed, 2 m temperature (the air temperature at 2 m above surface), total precipitation and the sum of rainfall for the previous seven days. Several studies have detected changes in Italian lakes linked to long term climate change and fluctuations in large scale regional climate drivers such as the North Atlantic Oscillation (NAO) and the East Atlantic pattern (EA) during winter [49, 50]. Daily values of the NAO (North Atlantic Oscillation) were taken from NOAA-CPC (<https://www.cpc.ncep.noaa.gov/products/precip/CWlink/pna/nao.shtml>).

For the analysis two approaches were trialed—Google AI (Auto ML) and Nonparametric Multiplicative Regression (NPMR). NPMR [51] was used to estimate the response of average daily Chl-a to climate and environmental parameters listed above. NPMR describes response surfaces using variables in a multiplicative instead of an additive way. This method is advanced and can better defining unimodal responses compared to methods such as multiple regression [51]. It has previously been applied to model tree species distribution [52], the response of lichens to climate change [53] and in time-series analysis [54]. NPMR was implemented with the software HyperNiche version 2.3 [55]. The Chl-a response was estimated with a local mean multiplicative smoothing function with Gaussian weighting. NPMR models were created by the stepwise adding of predictors with fit represented by a cross-validated R^2 (xR^2) which can be considered as a measure of fit similar to a traditional R^2 . The sensitivity, which is an indicator of the influence of each parameter included in the NPMR, was estimated by altering the range of predictors by $\pm 5\%$, with resulting deviations expressed as a proportion of the observed range of the response variable. Sensitivity can aid in comparing the importance of variables included in models because NPMR models are unlike standard linear regression having no fixed coefficients or slopes. Google AI (Auto ML) is a service that applies machine learning

models to diverse data types such as images, text, or numeric data aiming to automate the selection and application of models to data. Google AI (Auto ML) was also applied to produce a model for Chl-a as a designated feature. The supervised learning model followed a regression approach with chronological assignment using the first 80% of the timeseries for model training with each subsequent 10% used for validation (a fine-tuning of the models hyper parameters) and testing (with independent data deriving the model's performance statistics) (<https://cloud.google.com/automl-tables>). Both modeling approaches included the time component as the most important accounting for 87.3% as feature importance in Google AI and a combined (year and day of year) percentage sensitive value of 66.7% in NPMR. The next most important parameter was the NAO in both modelling approaches with a 3.9% feature importance in Google AI and 0.6% sensitivity in NPMR. No other parameters were included in the NPMR model while the Google AI approach estimated the seven day antecedent sum of rainfall as having a feature importance of 3.1% with no other variables accounting for more than 3%.

While a precise comparison is not possible between the two approaches owing to different model design and performance statistics they could be considered as broadly similar comparing the Google AI R^2 of 0.65 with that of the NPMR xR^2 of 0.54. A NPMR plot of Chl-a (as contour lines in Fig. 3.7) with NAO and the day of year (DOY) indicates that NAO appears to be most relevant to Chl-a concentration in the weeks around DOY 250 (7th September). More positive values of the NAO in early to mid-September were associated with higher Chl-a (Fig. 3.7). The importance of time in the models is likely linked to the consistency in timing of large September blooms over the years that dominate the seasonal pattern (Fig. 3.5). The size of these blooms is likely to be mostly determined by nutrients such as phosphorus given its key role in controlling algal populations [56]. Total phosphorus (TP) was not available at daily frequency for the lake but we can compare Chl-a concentration in early to mid-September with annual TP concentrations sourced from local authorities (<https://apps.arpa.umbria.it/acqua/Home>) and published values [26] (Fig. 3.8). The R^2 of the relationship was 0.65 indicating the strong influence of annual TP in determining

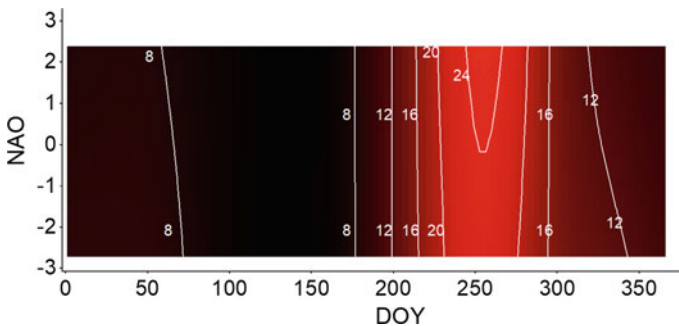
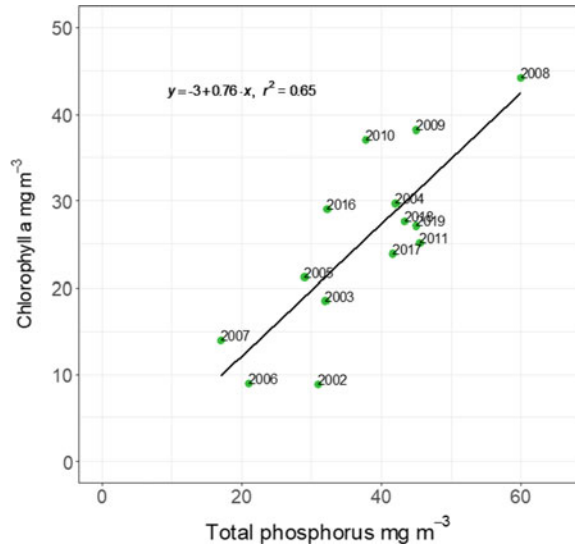


Fig. 3.7 Model estimates for Chl-a mg m^{-3} (contour lines) against DOY (Day of Year) and NAO (North Atlantic Oscillation)

Fig. 3.8 Chlorophyll-a (average of a two week period around day 250—7th September) and annual average total phosphorus



the size of the September phytoplankton bloom. In summary the analysis indicates that years with high TP concentrations and high NAO in early to mid-September, indicative of high pressure with warm sunny weather [57], will tend to lead to the largest phytoplankton blooms. The high temporal resolution of the CCI satellite data coupled with the ERA5 climatic data proved crucial to understanding the inter-annual dynamics driving phytoplankton blooms. It would not be possible to match the temporal and spatial coverage afforded by satellite monitoring with boat based sampling and laboratory analysis. However, such traditional methods are key to understanding providing TP and other nutrient concentrations and Chl-a data for validating satellite estimates.

The examination of the CCI timeseries for Chl-a indicated the importance of the temporal component and NAO for both AI and NPMR. While the importance of the temporal component reflects the regularity of the large blooms that dominate the annual pattern the influence of NAO was interesting. Previous work has identified the importance of winter values of teleconnection indices like the NAO and the EA where, for example, in deep sub-alpine lakes higher values lead to warmer winters preventing mixing and reducing nutrient supply from the hypolimnion [49, 50]. It has also been associated with controlling the onset of spring blooms and zooplankton abundance in some lakes [58]. In this study a higher NAO value in September was related to higher Chl-a and this may have resulted from higher temperatures and sunnier weather increasing cyanobacteria growth during this period. A meta-analysis of European lakes previously found summer cyanobacteria biomass to be associated with winter NAO which was attributed to a direct physiological influence of higher temperatures on growth or an increased period of stratification, although the latter would be irrelevant in the case of shallow Trasimeno likely to be more influenced by prevailing weather conditions [59]. As several species of cyanobacteria change

dominance during summer, the NAO may also influence the timing of the seasonal succession but this would require further analysis for confirmation.

The AI analysis also found the antecedent 7-day rain to be significant and this is likely to be indicative of the supply of nutrients to the lake. Examination of satellite images has previously identified phytoplankton blooms in the vicinity of an inflow to Trasimeno lake during summer that was followed by a widespread increase in Chl-a in the lake [19]. The good relationship between TP measured by local authorities and the average concentration of the September bloom, shows both how Chl-a is constrained by nutrients and also demonstrates the benefits of using satellite data to obtain a better temporal and spatial resolution.

3.5 Spaceborne Imaging Spectrometry

In recent years new spaceborne missions dedicated to hyperspectral measurements have been developed [60] and in this section imagery data acquired from PRISMA (Hyperspectral Precursor of the Application Mission) and DESIS (DLR Earth Sensing Imaging Spectrometer) are presented for assessing water quality in Lake Trasimeno.

PRISMA, a fully funded mission by the Italian Space Agency (ASI), is an EO system with innovative, electro-optical instrumentation that combines a hyperspectral sensor with a medium-resolution panchromatic camera. The PRISMA orbit is characterized by a revisit time in a nadir-looking configuration of 29 days, the system is capable of acquiring images distant 1000 km in a single pass (with a total rotation left to right side looking and vice versa) so that the temporal resolution can be improved significantly. The PRISMA Payload is composed of an Imaging Spectrometer, able to take images at 30 m resolution in a continuum of spectral bands ranging from 400 to 2500 nm, and a 5 m resolution Panchromatic Camera [61]. DESIS is a hyperspectral instrument integrated in the Multi-User-System for Earth Sensing (MUSES) platform installed on the International Space Station (ISS). The mission is operated by Teledyne Brown Engineering (TBE), Alabama, USA, and the German Aerospace Center (DLR), Germany. DESIS is realized as a pushbroom imaging spectrometer spectrally sensitive over the VNIR range from 400 to 1000 nm with a spectral sampling distance of 2.55 nm [62].

Within this study imagery data from PRISMA and DESIS of Lake Trasimeno acquired on the 25th July 2020 and on the 26th May 2020, respectively are used for water quality mapping. PRISMA data were downloaded as Level 1 (L1) products (top-of-atmosphere calibrated radiance), then imported and converted to ENVI format (L3Harris Technologies, Inc., Melbourne, FL, USA), re-projected with a geographic lookup table (GLT) Bowtie correction and re-scaled to physical units of $\text{mWcm}^{-2}\text{sr}^{-1} \mu\text{m}^{-1}$, in the case of DESIS the geocoded L1C products in ENVI format were simply re-scaled to physical units of $\text{mWcm}^{-2}\text{sr}^{-1} \mu\text{m}^{-1}$.

To map water quality, L1 PRISMA and DESIS imagery were firstly corrected for atmospheric effects in order to compute remote sensing reflectance R_{rs} . To this

aim, the ATCOR code (version 9.3.0, ATCOR-2 module) [63] was used as in Pepe et al. [64]. The code was pre-configured in order to handle data acquired from both sensors (e.g. spectral setting, swath) and then the correction was performed with varying visibility and water vapor, the related viewing and solar angles, a rural model for aerosols and by setting to 258 m above-sea-level the altitude of the target. The ATCOR-derived atmospherically corrected reflectance was then converted into remote sensing reflectance R_{rs} dividing by π . The ATCOR-derived R_{rs} values were compared to the WISPstation synchronous measurements (cf. Section 1). In particular, WISPstation data overlapping the sensing time of PRISMA within 15 min were averaged while, R_{rs} spectra of PRISMA and DESIS, were extracted from imagery data corresponding to a 3×3 pixel Region of Interest (ROI) centering the WISPstation position (cf. Figure 3.1). The comparison between spaceborne data and field measurements is shown in Fig. 3.9, that also includes the results of common descriptive statistical metrics (e.g., Bracaglia et al. [65]): root mean square difference (RMSD), spectral angle (SA), and the square of the coefficient of correlation (R^2) defined in the Table 3.1. The comparison of ATCOR-derived R_{rs} values with in situ measurements proved overall a very good agreement at all wavelengths. The magnitude and shape of PRISMA and DESIS are comparable to in situ data even if a more detailed examination of the peaks/dips seems to indicate a minor spectral shift of PRISMA.

In order to convert the R_{rs} data into biophysical water parameters such as Chl-a, Total Suspended Matter (TSM) and Colored Dissolved Organic Matter (CDOM) we

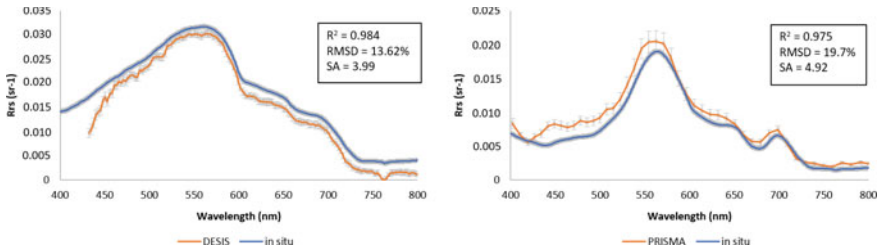


Fig. 3.9 Comparison between spectral signatures acquired by the WISPstation and obtained after atmospheric correction of DESIS (on the left) and PRISMA (on the right). The boxes contain the values of statistical metrics R^2 , RMSD and SA

Table 3.1 Statistical metrics used to assess the agreement of R_{rs} between spaceborne data and field measurements

Root mean square difference (RMSD)	$\sqrt{\frac{\sum_{i=1}^n (y_i - x_i)^2}{n}}$
Spectral angle (SA)	$\cos^{-1} \frac{\sum_{i=1}^n y_i x_i}{\sqrt{\sum_{i=1}^n y_i^2} \sqrt{\sum_{i=1}^n x_i^2}}$
Square of the coefficient of correlation (R^2)	$\frac{\sum_{i=1}^n (x_i - \bar{x})(y_i - \bar{y})}{\sqrt{\sum_{i=1}^n (x_i - \bar{x})^2} \sqrt{\sum_{i=1}^n (y_i - \bar{y})^2}}$

The values of statistical metrics RMSD, SA and R^2 are reported

used the BOMBER tool [66], which implements a non-linear optimisation procedure to derive water parameters from a four-component bio-optical model. To this aim the bio-optical model was parameterized with the specific inherent optical properties of Lake Trasimeno as described in Giardino et al. [67].

For Chl-a we can compare the image products from PRISMA and DESIS with in situ data collected by ARPA Umbria on the 25th May 2020 and 20th July 2020. The Chl-a concentrations were measured from samples collected from the euphotic zone at two WFD stations named Center and San Feliciano (Fig. 3.1). Chl-a concentration was then determined in the laboratory spectrophotometrically (using acetone 90% for the extraction) and calculated following Lorenzen [68]. The results of the comparison show a good agreement between hyperspectral-derived products (for which the standard deviation can be also computed over the 3×3 ROI) and laboratory measurements. In particular, on the 26th May 2020: in situ data were 2.8 and 4 mg m^{-3} (respectively for stations TRS30 and TRS35) with corresponding values from DESIS of 2.9 ± 0.3 and $3.8 \pm 0.5 \text{ mg m}^{-3}$. On the 25th July 2020, in situ data were 18.7 and 13.2 mg m^{-3} (respectively for stations TRS30 and TRS35), with corresponding values from PRISMA of $19.7 \pm 0.6 \text{ mg m}^{-3}$ (st.dev 0.6) and $12.5 \pm 1.7 \text{ mg m}^{-3}$.

Figures 3.10 and 3.11 show the true-color composite and products obtained from DESIS and PRISMA, nicely depicting the ranges of concentrations and spatial patterns in Lake Trasimeno. Overall the DESIS map of spring 2020 shows rather turbid conditions, with TSM concentration reaching 20 g m^{-3} . In contrast, Chl-a concentrations remain rather low (maximum of 8 mg m^{-3}), while the absorption due to CDOM is between 0 and 1 m^{-1} . In the case of the PRISMA image, the mapping indicates more productive waters typical of the summer season, with Chl-a concentrations reaching 30 mg m^{-3} . In this case TSM and CDOM are lower than 10 g m^{-3} and 0.5 m^{-1} respectively, indicating a dominance of phytoplankton with respect to the other water components. By comparing DESIS and PRISMA products, as well as the true-color composite, it is also evident how the region characterised by the presence of aquatic vegetation in the south-east bay of Lake Trasimeno, covers a greater area in the PRISMA scene compared to the DESIS. This localized feature is consistent with the seasonal changes in macrophyte abundance. In late May, at the time of DESIS image acquisition, the aquatic plants have just started their phenological cycle; compared to late July, at the time of the PRISMA image when all plants are much more developed. In addition, this will influence water conditions, since the macrophyte community tends to keep the water clearer, therefore the TSM concentrations from DESIS are higher than those observed by PRISMA.

3.6 High Spatial Resolution Products

High spatial resolution images (<5 m pixel resolution from e.g. WorldView, Rapid-Eye, PlanetScope) are typically designed for terrestrial applications, nevertheless these sensors can have aquatic applications whenever finer scale mapping is needed

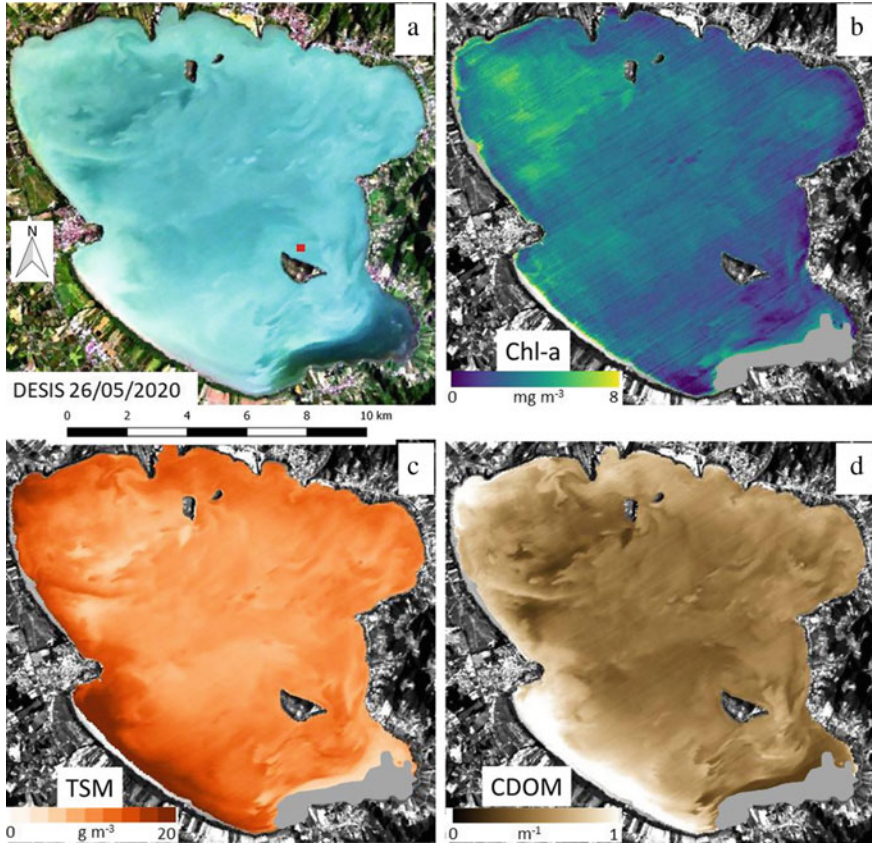


Fig. 3.10 The pseudo true colour DESIS image acquired on 26th May 2020 and the three BOMBER-retrieved products. The lake area with substrates colonized by aquatic vegetation (in grey) in the Oasi la Valle bay (cf. Fig. 3.1) are masked as BOMBER was run for optically deep waters only

(e.g., Giardino et al. [69], Niroumand-Jadidi [70] for water constituents; and e.g. Doxani et al. [71], Arsen [72], Halls and Costin [73] for macrophyte mapping and coastal bathymetry). High spatial resolution satellite data is often preferable to medium-to-low spatial resolution data, for example, when the ecosystems include small macrophyte stands, when macrophyte community expansion or recession occurs over a few square meters, or whenever fine-scale mapping is required to support proper management decisions. In such situations, it is important to remember that high spatial resolution images are usually acquired on demand by commercial entities and it will be necessary to obtain a quote in advance for the service. Moreover the data may be challenging due to a high variation of sensor angles and a signal to noise ratio not optimised for aquatic applications [74].

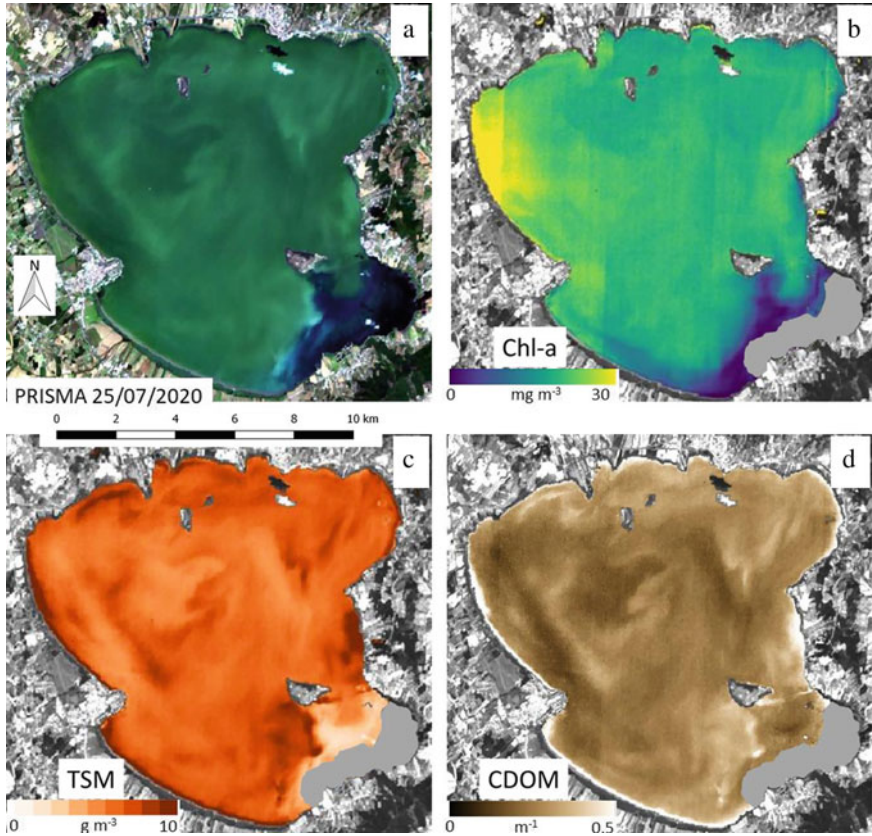


Fig. 3.11 The pseudo true colour PRISMA image acquired on 25th July 2020 and the three BOMBER-retrieved products. The lake area with substrates colonized by aquatic vegetation (in grey) in the Oasi la Valle bay (cf. Fig. 3.1) are masked as BOMBER was run for optically deep waters only

In the case of Lake Trasimeno, the use of high spatial resolution satellite images was previously investigated to obtain information on the status and changes of macrophyte communities, that are unfortunately showing a slight deterioration. In particular, *Potamogeton* associations declined by about 20% from 2003 to 2008 [27]. Moreover, the progressive dieback of the common reed [75] on the lake littoral occurred with a loss of about 66% of its total surface area in the period between 1988 and 2005 [75, 76]. The macrophyte decrease is mostly attributable to an increase of water turbidity, even if some fish species (such as goldfish, common carp and grass carp) that are prospering in the lake, can eat significant quantities of vegetation [77]. The invasive red swamp crayfish (*Procambarus clarkia*) and coypu (*Myocastor coypus*) might have also contributed to the macrophyte decline in Lake Trasimeno, due to their feeding habits [78, 79]. Previous work tracing a period of decline in

common reed health has used different high spatial resolution images (QuickBird, ASTER and ALOS-AVNIR/2) by Bresciani et al. [80].

In this study, an example of the use of high spatial resolution satellite data is shown to estimate the portion of Lake Trasimeno covered by submerged macrophytes (with also a subdivision of the type of association of macrophytes present) and to assess whether there have been changes over time. To the aim, data have been gathered from the WorldView-3 multispectral satellite sensor, launched in 2014, with a spatial resolution at nadir at 1.24 m having 8 bands in the region from 400 to 1040 nm. The WordView-3 image of Lake Trasimeno was acquired on the 4th August 2019 and it was atmospherically corrected with Simulation of the Satellite Signal in the Solar Spectrum vector code (6SV) [81, 82]. Then, the bio-optical model BOMBER [66] parametrized with specific inherent optical properties of Lake Trasimeno [67] was used to estimate bottom types from imagery data. Before to run the bio-optical model we applied a Normalized Difference Water Index (NDWI) to maps the presence of common reed and emergent macrophytes area according to Lantz and Wang [83]. The bottom type map (Fig. 3.12) shows the main association of submerged macrophytes growing in the Oasi La Valle, in the southern-east part of Lake Trasimeno (cf. Fig. 3.1). The map in red and green tones shows areas dominated by dense submerged macrophyte stands. Although this area is still rather extended, a decrease of about 100 hectares of submerged macrophytes is observed when compared to the same period of 2014 [67].

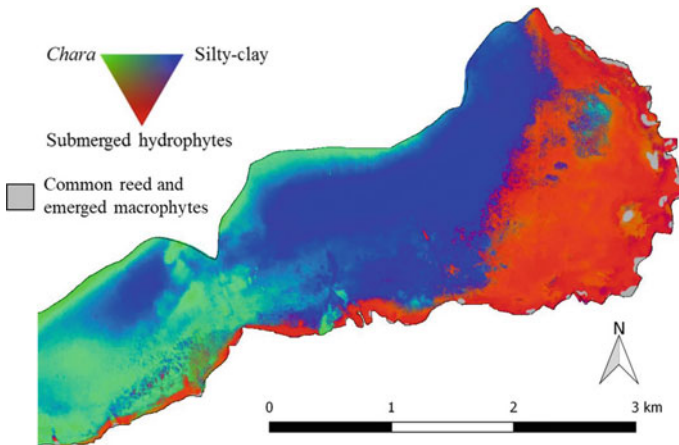


Fig. 3.12 Map of the benthic substrate and submerged macrophytes in the southern eastern portion of the Lake Trasimeno (Oasi La Valle site) retrieved by WordView-3 image acquired on the 4th August 2019. In grey the common reed and emergent macrophytes

3.7 Conclusions

This work demonstrates that remote and proximal sensing data can provide accurate and high-resolution information for water monitoring and management and extend the scientific understanding of Lake Trasimeno. The integrated and multi-scale approach (combining sources from field, fixed station and multiple satellites) to assessing Chl-a and other water quality parameters has the benefit of improving confidence, knowledge and substantially increases the potential for research, monitoring and model development.

High temporal and spectral resolution spectroradiometric data, such as those obtained by WISPstation in Lake Trasimeno, allows the estimation of phytoplankton pigment concentration and in particular to identify the start and rate of increase of the summer bloom. The phenology was found to be consistent in the three years investigated (2018–2020), with a bloom typically increasing between the 29th June–7th September and a slope ranging from 0.50 to 0.59. Moreover, PC retrieval demonstrated that cyanobacteria played a pivotal role in the sudden increases and declines in Chl-a in mid to late summer. For water managers, one of the benefits of the use of the WISPstation data is the coupling of the retrieval of different pigments that allows the identification of different phytoplankton functional groups and the detection, in almost real time, of potentially toxic cyanobacteria. Coupling high frequency (hourly) and temporal (daily, seasonal) data helped to develop understanding, giving clear benefits for water management in detecting and predicting bloom event dynamics and manifestation. A drawback is that the WISPstation is limited to a fixed position and describes a point-like portion of the lake; a gap that can be successfully filled with the satellite technology.

The availability of long time-series of satellite observations for different parameters, such as LSWT, Chl-a and turbidity from the recent ESA CCI Lakes database [48] allowed a clear view over time showing that the peak height of the algal blooms increased from 2008 onwards. Moreover, the performed analysis suggested that years with high TP concentrations and high NAO in early to mid-September, indicative of high nutrient availability with warm sunny weather, will tend to lead to the largest phytoplankton blooms. Currently the lake is classified as eutrophic and periodic blooms can interfere with the recreational use and tourism in the lake area. Therefore, long-time series of satellite-derived maps allow the examination of the phenology and intensity of phytoplankton bloom history, an opportunity to identify drivers of the long-term dynamics in communities which is a complex subject as it may consist of several factors acting in parallel and it is also an opportunity for managers to identify hotspot zones that tend to show higher bloom events.

With the CCI dataset set to expand to 2000 lakes in the second phase of the project it will represent an important resource for the scientific community and water quality managers.

The new generation of satellite hyperspectral data (i.e., PRISMA, DESIS) among other things, offers the opportunity for high quality spatial data on water quality.

The comparison between spaceborne Rrs data and field measurements (by WISPstation) shown a good agreement ($R^2 = 0.98$) as did the comparison between Chl-a hyperspectral-derived products and Chl-a laboratory measurements. DESIS derived maps of spring 2020 shown that Lake Trasimeno was characterized by high turbidity ($TSM > 20 \text{ gm}^{-3}$) and low Chl-a concentration (up to 8 mg m^{-3}) and low presence of aquatic vegetation. Instead, in summer the PRISMA-derived maps indicated more productive waters ($\text{Chl-a} > 30 \text{ mg m}^{-3}$), and low turbidity ($TSM < 10 \text{ g m}^{-3}$) influenced by the presence of submerged vegetation in the southern-east part of the lake which favors increased water transparency.

Another important aspect to be considered is the availability of high resolution spatial data in supporting specific analysis on primary producers, such as hotspots of algal blooms and submerged macrophytes cover and abundance. On this last issue, in this study an example of the use of high spatial resolution satellite data (WorldView-3 with 1.2 m pixel resolution) was shown to estimate the portion of Lake Trasimeno covered by submerged macrophytes (with also a subdivision of the type of association of macrophytes) and to assess whether there have been changes over time. In fact, the bottom type map produced (2019) shown a decrease of submerged macrophytes compared to the same period of 2014.

The different approach applied in this work may be transferred to other water bodies to analyze specific features of phytoplankton species, which can threaten the conservation of aquatic habitats and interfere with human recreational activities (e.g. touristic navigation, fishing), thus heavily impacting on the ecosystem and socio-economics.

Overall, this study confirms how advanced remote sensing technology is continuously providing enhanced opportunities to monitor changes in space and time and to perform retrospective analysis of water quality status. Integrated data from different optical sensors are also a key element because such an approach allows, upon verification of the methods and accuracies, the continuity of consistent analysis of water quality, and guarantees a support to decision-makers involved in monitoring, management and conservation of aquatic ecosystems.

Acknowledgements This research is co-funded by ESA CCI LAKES project (GA n. 40000125030/18/I-NB) and by the Italian Space Agency with PRISCAV project (grant nr. 2019-5-HH.0) and by the H2020 EOMORES project (GA n. 730066) for the WISPstation. We would like to thank the “Cooperativa dei Pescatori del Trasimeno” for the support in field campaigns. Many thanks to Alessandra Cingolani, Fedra Charavgis and Valentina DellaBella from ARPA Umbria for useful discussions on research results. We are grateful to Luca Nicoletti and Luca Galli from ARPA Umbria for collecting water samples. We also thank the Province of Perugia for the availability to use the platform in Polvese Island used for the WISPstation. We are very grateful to Ettore Lopinto from ASI and to Uta Heiden and Nicole Pinnel from DLR for valuable discussions on PRISMA and DESIS products respectively.

References

1. Organisation for Economic Co-operation and Development (2001) OECD environmental strategy for the first decade of the 21st Century: adopted by OECD environmental ministers. OECD
2. Giovannini E (2008) Understanding economic statistics: an OECD perspective. OECD, Paris
3. Coicaud JM, Zhang J (2011) The OECD as a global data collection and policy analysis organization: some strengths and weaknesses. *Global Pol* 2(3):312–317
4. Directive (2000) Directive 2000/60/EC of the European Parliament and of the council of 23 October 2000 establishing a framework for community action in the field of water policy. *Off J Europ Commun* L327:1–72
5. Garrote L (2017) Managing water resources to adapt to climate change: facing uncertainty and scarcity in a changing context. *Water Resour Manage* 31(10):2951–2963
6. Carvalho L, Mackay EB, Cardoso AC, Baattrup-Pedersen A, Birk S, Blackstock KL, Borics G, Borja A, Feld CK, Ferreira MT, Globevnik L (2019) Protecting and restoring Europe's waters: an analysis of the future development needs of the water framework directive. *Sci Total Environ* 658:1228–1238
7. Woolway RI, Kraemer BM, Lenters JD, Merchant CJ, O'Reilly CM, Sharma S (2020) Global lake responses to climate change. *Nat Rev Earth Environ* 1(8):388–403
8. Williamson CE, Saros JE, Vincent WF, Smol JP (2009) Lakes and reservoirs as sentinels, integrators, and regulators of climate change. *Limnol Oceanogr* 54:2273–2282
9. Adrian R, O'Reilly CM, Zagarese H, Baines SB, Hessen DO, Keller W, Livingstone DM, Sommaruga R, Straile D, Van Donk E, Weyhenmeyer GA (2009) Lakes as sentinels of climate change. *Limnol Oceanogr* 54(6):2283–2297
10. Bukata RP, Jerome JH, Kondratyev KY, Pozdnyakov DV (1991) Satellite monitoring of optically-active components of inland waters: an essential input to regional climate change impact studies. *J Great Lakes Res* 17(4):470–478
11. Yang J, Gong P, Fu R, Zhang M, Chen J, Liang S, Xu B, Shi J, Dickinson R (2013) The role of satellite remote sensing in climate change studies. *Nat Clim Chang* 3(10):875–883
12. Hu C, Lee Z, Ma R, Yu K, Li D, Shang S (2010) Moderate resolution imaging spectroradiometer (MODIS) observations of cyanobacteria blooms in Taihu Lake, China. *J Geophys Res: Oceans* 115(C4)
13. Tyler AN, Hunter PD, Spyrakos E, Groom S, Constantinescu AM, Kitchen J (2016) Developments in Earth observation for the assessment and monitoring of inland, transitional, coastal and shelf-sea waters. *Sci Total Environ* 572:1307–1321
14. Odermatt D, Gitelson A, Brando VE, Schaepman M (2012) Review of constituent retrieval in optically deep and complex waters from satellite imagery. *Remote Sens Environ* 118:116–126
15. Ogashawara I, Mishra DR, Mishra S, Curtarelli MP, Stech JL (2013) A performance review of reflectance based algorithms for predicting phycocyanin concentrations in inland waters. *Remote Sens* 5(10):4774–4798
16. Gholizadeh MH, Melesse AM, Reddi LA (2016) Comprehensive review on water quality parameters estimation using remote sensing techniques. *Sensors* 16:1298
17. Greb S, Dekker AG, Binding C, Bernard S, Brockmann C, DiGiacomo P, Griffith D, Groom S, Hestir E, Hunter P, Kutser T (2018) Earth observations in support of global water quality monitoring. International Ocean-Colour Coordinating Group
18. Kutser T, Hedley J, Giardino C, Roelfsema C, Brando VE (2020) Remote sensing of shallow waters—a 50 year retrospective and future directions. *Remote Sens Environ* 240:111619
19. Bresciani M, Pinaridi M, Free G, Luciani G, Ghebrehiwot S, Laanen M, Giardino C et al (2020) The use of multisource optical sensors to study phytoplankton spatio-temporal variation in a Shallow Turbid Lake. *Water* 12(1):284
20. Taticchi MI (1992) Studies on Lake Trasimeno and other water bodies in Umbria Region (Central Italy). In: Guilizzoni P, Tartari G, Giussani G (eds) *Limnology in Italy*. Tipografia Griggi, Baveno, Italy, pp 295–317

21. Carosi A, Ghetti L, Padula R, Lorenzoni M (2019) Potential effects of global climate change on fisheries in the Trasimeno Lake (Italy), with special reference to the goldfish *Carassius auratus* invasion and the endemic southern pike *Esox cisalpinus* decline. *Fish Manage Ecol* 26(6):500–511
22. Deffenu L, Dragoni W (1978) Idrogeologia del Lago Trasimeno. *Geologia Applicata e Idrogeologia* 13:11–67
23. Dragoni W (2004) Il Lago Trasimeno e le variazioni climatiche (in Italian with English transl.) Provincia di Perugia, 60 pp
24. Frondini F, Dragoni W, Morgantini N, Donnini M, Cardellini C, Caliro S, Chiodini G et al (2019) An Endorheic Lake in a changing climate: geochemical investigations at Lake Trasimeno (Italy). *Water* 11(7):1319
25. Ludovisi A, Gaino E, Bellezza M, Casadei S (2013) Impact of climate change on the hydrology of shallow Lake Trasimeno (Umbria, Italy): history, forecasting and management. *Aquat Ecosyst Health Manage* 16(2):190–197
26. Ludovisi A, Gaino E (2010) Meteorological and water quality changes in Lake Trasimeno (Umbria, Italy) during the last fifty years. *J Limnol* 69(1):174–188
27. Giardino C, Bresciani M, Villa P, Martinelli A (2010) Application of remote sensing in water resource management: the case study of Lake Trasimeno, Italy. *Water Res manag* 24(14):3885–3899
28. Cingolani A, Charavgis F (2017) Valutazione dello stato ecologico e chimico dei corpi idrici lacustri (2013–2015). ARPA Umbria Technical report, 25 pp
29. Havens KE, Elia AC, Taticchi MI, Fulton RS (2009) Zooplankton–phytoplankton relationships in shallow subtropical versus temperate lakes Apopka (Florida, USA) and Trasimeno (Umbria, Italy). *Hydrobiologia* 628(1):165–175
30. Salmaso N (2010) Long-term phytoplankton community changes in a deep subalpine lake: responses to nutrient availability and climatic fluctuations. *Freshw Biol* 55:825–846
31. Lorenzoni M, Dolciami R, Ghetti L, Pedicillo G, Carosi A (2010) Fishery biology of the goldfish *Carassius auratus* (Linnaeus, 1758) in Lake Trasimeno (Umbria, Italy). *Knowl Manag Aquat Ecosyst* 396:01
32. Coesel PFM, Kwakkestein R, Verschoor A (1978) Oligotrophication and eutrophication tendencies in some Dutch moorland pools, as reflected in their desmid flora. *Hydrobiologia* 61:21–31
33. Pernthaler A, Pernthaler J (2005) Diurnal variation of cell proliferation in three bacterial taxa from coastal North Sea waters. *Appl Environ Microbiol* 71:4638–4644
34. Ruiz-González C, Lefort T, Massana R, Simó R, Gasol JM (2012) Diel changes in bulk and single-cell bacterial heterotrophic activity in winter surface waters of the northwestern Mediterranean Sea. *Limnol Oceanogr* 57:29–42
35. Ezra AG, Nwankwo DI (2001) Composition of phytoplankton algae in Gubi Reservoir, Bauchi, Nigeria. *J Aquat Sci* 16(2):115–118
36. Peters S, Laanen M, Groetsch P, Ghezehegn S, Poser K, Hommersom A, De Reus E, Spaais L (2018) WISP station: a new autonomous above water radiometer system. In: Proceedings of the ocean optics XXIV conference. Dubrovnik, Croatia, 7–12 October 2018
37. Giardino C, Bresciani M, Braga F, Fabbretto A, Ghirardi N, Pepe M, Brando VE et al (2020) First evaluation of PRISMA level 1 data for water applications. *Sensors* 20(16):4553
38. Gons HJ (1999) Optical teledetection of chlorophyll a in turbid inland waters. *Environ Sci Technol* 33:1127–1132
39. Simis S (2006) Blue-green catastrophe: remote sensing of mass viral lysis of cyanobacteria. Ph.D. Thesis, Vrije University, Amsterdam
40. Wolfram G, Argillier C, de Bortoli J, Buzzi F, Dalmiglio A, Dokulil MT et al (2009) Reference conditions and WFD compliant class boundaries for phytoplankton biomass and chlorophyll-a in Alpine lakes. *Hydrobiologia* 633:45–58
41. Pinheiro J, Bates D, DebRoy S, Sarkar D, Team RC (2013) nlme: Linear and nonlinear mixed effects models. *R Package Version* 3(1):111
42. Lenth RV (2016) Least-squares means: the R package lsmeans. *J Stat Softw* 69:1–33

43. R Core Team (2019) R: a language and environment for statistical computing. Vienna. R Foundation for Statistical Computing, Austria. <https://www.R-project.org/>
44. Charavgis F, Cingolani A, Di Brizio M, Tozzi G, Rinaldi E, Stranieri P (2018) Qualita' delle acque di balneazione dei laghi Umbri. ARPA, Umbria
45. Funari E, Manganelli M, Buratti FM, Testai E (2017) Cyanobacteria blooms in water: Italian guidelines to assess and manage the risk associated to bathing and recreational activities. *Sci Total Environ* 598:867–880
46. Hamilton DP, Carey CC, Arvola L, Arzberger P, Brewer C, Cole JJ, Gaiser E, Hanson PC, Ibelings BW, Jennings E (2015) A Global lake ecological observatory network (GLEON) for synthesising high-frequency sensor data for validation of deterministic ecological models. *Inland Waters* 5:49–56
47. Charavgis F, Cingolani A, Di Brizio M, Rinaldi E, Tozzi G, Stranieri P (2020) Qualita' delle acque di balneazione dei laghi Umbri, stagione balneare 2019. ARPA, Umbria
48. Crétaux J-F, Merchant CJ, Duguay C, Simis S, Calmettes B, Bergé-Nguyen M, Wu Y, Zhang D, Carrea L, Liu X, Selmes N, Warren M (2020) ESA Lakes climate change initiative (Lakes_cci): Lake products, Version 1.0. centre for environmental data analysis, 08 June 2020
49. Rogora M, Buzzi F, Dresti C, Leoni B, Lepori F, Mosello R et al (2018) Climatic effects on vertical mixing and deep-water oxygen content in the subalpine lakes in Italy. *Hydrobiologia* 824(1):33–50
50. Salmaso N, Boscaini A, Capelli C, Cerasino L (2018) Ongoing ecological shifts in a large lake are driven by climate change and eutrophication: evidences from a three-decade study in Lake Garda. *Hydrobiologia* 824(1):177–195
51. McCune B (2006) Nonparametric multiplicative regression for habitat modeling. Oregon State University, Oregon
52. Yost AC (2008) Probabilistic modeling and mapping of plant indicator species in a Northeast Oregon industrial forest, USA. *Ecol Ind* 8(1):46–56
53. Ellis CJ, Coppins BJ, Dawson TP, Seaward MR (2007) Response of British lichens to climate change scenarios: trends and uncertainties in the projected impact for contrasting biogeographic groups. *Biol Cons* 140(3–4):217–235
54. Nicolaou N, Constantinou TG (2016) a nonlinear causality estimator based on non-parametric multiplicative regression. *Front Neuroinf* 10
55. McCune B, Mefford MJ (2009) HyperNiche. In: Nonparametric multiplicative habitat modeling. MjM Software, Oregon, USA
56. Sakamoto M (1966) Primary production by phytoplankton community in some Japanese lakes and its dependence on lake depth. *Arch Hydrobiol* 62:1–28
57. Criado-Aldeanueva F, Soto-Navarro J (2020) Climatic Indices over the Mediterranean Sea: a review. *Appl Sci* 10(17):5790
58. Gerten D, Adrian R (2000) Climate-driven changes in spring plankton dynamics and the sensitivity of shallow polymictic lakes to the North Atlantic Oscillation. *Limnol Oceanogr* 45(5):1058–1066
59. Blenckner T, Adrian R, Livingstone DM, Jennings E, Weyhenmeyer GA, George DG et al (2007) Large-scale climatic signatures in lakes across Europe: a meta-analysis. *Glob Change Biol* 13(7):1314–1326
60. Rast M, Painter TH (2019) Earth observation imaging spectroscopy for terrestrial systems: An overview of its history, techniques, and applications of its missions. *Surv Geophys* 40:303–331
61. Loizzo R, Guarini R, Longo F, Scopa T, Formaro R, Facchinetti C, Varacalli G (2018) PRISMA: the Italian hyperspectral mission. In: Proceedings of the international geoscience and remote sensing symposium on observing, understanding and forecasting the dynamics of our planet (IGARSS). Valencia, Spain, 22–27 July 2018
62. Alonso K, Bachmann M, Burch K, Carmona E, Cerra D, de los Reyes R, Dietrich D, Heiden U, Holderlin A, Ickes J et al (2019) Data products, quality and validation of the DLR Earth sensing imaging spectrometer (DESI). *Sensors* 19:4471
63. Richter R, Schläpfer D (2018) Atmospheric/topographic correction for satellite imagery (ATCOR-2/3 User Guide, Version 9.3. ReSe Applications Schläpfer, Langeggweg, 3

64. Pepe M, Pompilio L, Gioli B, Busetto L, Boschetti M (2020) Detection and classification of non-photosynthetic vegetation from PRISMA hyperspectral data in croplands. *Remote Sensing* 12:3903
65. Bracaglia M, Santoleri R, Volpe G, Colella S, Benincasa M, Brando VE (2020) A virtual geostationary ocean color sensor to analyze the coastal optical variability. *Remote Sensing* 12:1539
66. Giardino C, Candiani G, Bresciani M, Lee Z, Gagliano S, Pepe M (2012) BOMBER: a tool for estimating water quality and bottom properties from remote sensing images. *Comput Geosci* 45:313–318
67. Giardino C, Bresciani M, Valentini E, Gasperini L, Bolpagni R, Brando VE (2015) Airborne hyperspectral data to assess suspended particulate matter and aquatic vegetation in a shallow and turbid lake. *Remote Sens Environ* 157:48–57
68. Lorenzen CJ (1967) Determination of chlorophyll and phaeo-pigments: spectrophotometric equations. *Limnol Oceanogr* 12:343–346
69. Giardino C, Bresciani M, Cazzaniga I, Schenk K, Rieger P, Braga F, Matta E, Brando VE (2014) Evaluation of multi-resolution satellite sensors for assessing water quality and bottom depth of Lake Garda. *Sensors* 14(12):24116–24131
70. Niroumand-Jadidi M, Bovolo F, Bruzzone L, Gege P (2020) Physics-based bathymetry and water quality retrieval using planetscope imagery: Impacts of 2020 Covid-19 lockdown and 2019 extreme flood in the Venice Lagoon. *Remote Sens* 12(15):2381
71. Doxani G, Papadopoulou M, Lafazani P, Pikridas C, Tsakiri-Strati M (2012) Shallow-water bathymetry over variable bottom types using multispectral Worldview-2 image. *Int Archives Photogrammetry, Remote Sens Spatial Inf Sci* 39(8):159–164
72. Arsen A, Crétaux JF, Berge-Nguyen M, Del Rio RA (2014) Remote sensing-derived bathymetry of lake Poopó. *Remote Sensing* 6(1):407–420
73. Halls J, Costin K (2016) Submerged and emergent land cover and bathymetric mapping of estuarine habitats using worldView-2 and LiDAR imagery. *Remote Sensing* 8(9):718
74. Fisher JR, Acosta EA, Dennedy-Frank PJ, Kroeger T, Boucher TM (2018) Impact of satellite imagery spatial resolution on land use classification accuracy and modeled water quality. *Remote Sens Ecol Conserv* 4(2):137–149
75. Gigante D, Landucci F, Truffini A, Venanzoni R (2013) Phytosociological and ecological features of a dying-back reed bed at the Lake Trasimeno (central Italy). *Archives Geobotany* 14(1–2):81–89
76. Gigante D, Venanzoni R, Zuccarello V (2011) Reed die-back in southern Europe? a case study from Central Italy. *CR Biol* 334(4):327–336
77. Sheffer M (1998) Ecology of shallow lakes. Chapman & Hall, London, UK
78. Prigioni C, Balestrieri A, Remonti L (2005) Food habits of the coypu, *Myocastor coypus*, and its impact on aquatic vegetation in a freshwater habitat of NW Italy. *Folia Zool* 54(3):269–277
79. Souty-Grosset C, Anastácio PM, Aquiloni L, Banha F, Choquer J, Chucholl C, Tricarico E (2016) The red swamp crayfish *Procambarus clarkii* in Europe: impacts on aquatic ecosystems and human well-being. *Limnologica* 58:78–93
80. Bresciani M, Stroppiana D, Fila G, Montagna M, Giardino C (2009) Monitoring reed vegetation in environmentally sensitive areas in Italy. *Italian J Remote Sens* 41(2):125–137
81. Vermote EF, Tanré D, Deuze JL, Herman M, Morcette JJ (1997) Second simulation of the satellite signal in the solar spectrum, 6S: an overview. *IEEE Trans Geosci Remote Sens* 35(3):675–686
82. Kotchenova SY, Vermote EF, Matarrese R, Klemm FJ Jr (2006) Validation of a vector version of the 6S radiative transfer code for atmospheric correction of satellite data. Part I: path radiance. *Appl Opt* 45(26):6762–6774
83. Lantz NJ, Wang J (2013) Object-based classification of Worldview-2 imagery for mapping invasive common reed, *Phragmites australis*. *Can J Remote Sens* 39(4):328–340